MODIS Science Team Member

Semi-Annual Report

(Jan - Jun 2001)

Eric Vermote (University of Maryland) – Science Team Member

John O' Bannon (UMD), Rhonda Davis (UMD), Francois PetitColin (UMD), James Ray (SSAI), Nazmi El Saleous (RSTX),

Contract: NAS5-96062

A. FOCUS ACTIVITIES DURING THE REPORTING PERIOD

The most important activities undertaken during this reporting period are the following:

1. Land surface reflectance code development, testing and delivery
2. Internal filtering masks development (cloud, fire, snow)
3. MODIS Middle Infrared surface reflectance
4. MODIS Adaptive Processing System (MODAPS)/PI Processing/250m system

1. Land surface reflectance code development, testing and delivery

Several corrections were done to the code for generating level 2, Level 3 land surface reflectance and thermal anomaly products (MOD_PR09, or PGE 11).

1.1 Thermal Anomalies

The development of a separate program for thermal anomaly products (Louis Giglio, SSAI) allows us to eliminate thermal anomaly calculation from PGE11. To this end, as a first step we made sure PGE11 could work when the thermal anomaly product is turned off; we found that current versions of the program will not work in this case. However, attempts to run PGE11 without generating the thermal anomaly product coincided with several operating system changes on tracer (the main MODIS land product software development system), which made program development on tracer particularly difficult. A version of PGE11 that worked well with or without the generation of thermal anomaly products was therefore developed on modland, and then ported to tracer.

1.2 Polarization Correction

The code was obtained to be used in polarization correction of radiance data from Jim Brown (U. of Miami), and a standalone program was developed which applies polarization correction to radiance data values for inclusion in PGE11 code, and efforts on improving the performance of the program have been implemented. Finally after the first validation against the Miami code and independent evaluation, the polarization correction algorithm and look-up tables (Jim Brown, U. of Miami) were added to our code.

1.3 Internal masks

We worked on replacing data from bad detectors in band 26 with interpolated values from adjacent detectors, we improved the internal cloudmask by comparing band 20 reflectance to band 7 reflectance. The band 20 reflectance calculation (including transmission terms), the internal cloud mask (use of 1 km data, different thresholds), and aerosol retrieval (using band 26 as cirrus cloud flag) fine-tuned. Too, we tested the new aerosol retrieval version of PGE11 extensively on the main MODIS land product software development system.

1.4 Bug fixes/ Improvement to atmospheric correction

Corrections were implemented for inconsistent encoding of the year in NCEP ancillary input files, for inconsistent scaling of bands 20, 31 and 32, and for seasonal variations in Earth-sun distance in the atmospheric correction, as well a fix making 250m data aggregation dependent upon L1B file version. We improved the processing of NCEP ancillary data, and added the option of reading air temperature from NCEP files, which improved the overall performance of program. We considered alternatives to the use of 5-minute ETOPO data as a source of high-resolution topography, and added the ability of PGE11 to read elevation data from MOD03. Too, we added to the aerosol retrieval algorithm the retrieval of aerosols over water.

1.5 Metadata / MCF's

We obtained new metadata configuration files (MCFs) for the new collection (collection 3) and for reprocessing; for PGE11 we made all the required code changes for collection 3 to the aerosol retrieval version of the PGE11 code.

1.6 Level 3 surface reflectance

In regards to the code for generating level 3 composites of land surface reflectance (MOD_PR09A, or PGE21), we obtained new metadata configuration files (MCFs) for the new collection (collection 3) and for reprocessing and made all the required code changes for collection 3. We added last-minute changes to its 250m compositing algorithm, which provided the finishing touches on improvements to PGE21's performance. We updated all file specs, history files, etc, and delivered the collection 3 version of PGE21 (version 3.0.0) to the software testing and integration group (STIG). We added Aqua compatibility to PGE21. PGE21's science code itself was fully capable of processing Aqua data already, but it would add Terra-specific metadata to the outputs because Aqua-specific metadata configuration files (MCFs) were not available. Aqua-specific MCFs were written; the code was adapted to check the MCFs and ensure consistency among the MCFs, the PCF and the input files in order to prevent mixing of Terra and Aqua data.

2. Development and implementation of collection 3 algorithms

Following the preceding development (see previous report), a new approach has been determined to generate the aerosol product at 1km resolution and over bright targets. The new algorithm has pointed out to other area of possible improvements in the cloud mask, snow mask, sun-glint and fire. Basically in those situations a reliable aerosol optical thickness cannot be derived and they need to be identified carefully by the algorithm in order to be filtered out. Since we also are not using MOD04, which included the aerosol over water as input, an aerosol retrieval and correction over water also had to be implemented. Our focus was mainly to develop the ability to derive and correct aerosol over inland and coastal water but not for open ocean. We have developed a specific module that uses the reflectance at 3.75mic (band 20 and 21), the cirrus band (band 26), an estimate of surface temperature based on the split window technique (band 31 and 32), an estimate of the air-temperature at the time of MODIS acquisition from NCEP data and some simple spectral indices based on the MODIS reflectance band 1 to 7 corrected for molecular scattering and gaseous absorption to classified the pixels into clear, cloudy, snow, sun-glint, fire, and turbid water category. In those cases, no aerosol retrieval is performed and the values used for aerosol optical depth are derived from interpolation of valid retrievals.

2.1 Internal cloud mask

The internal cloud mask relies on two reflective tests, coupled with a thermal test for robustness. The reflective tests are only based in the short wave and middle infrared data combined as an index called the middle infrared anomaly to avoid the confusion between heavy aerosol and clouds; the thermal test enables us to rule out cases where the middle infrared reflectance anomaly is high (fires, sun-glint and to a certain extent bright surfaces). The middle infrared reflectance anomaly is defined as:

$$MIRA = \rho_{20,21} - 0.82\rho_7 + 0.32\rho_6 \quad (1)$$

The reflectance in band 20 and 21 is derived operationally for internal masking purposes using the semi-empirical approach described in (Roger and Vermote, 1998), which is validated by comparison to the rigorous approach described in (PetitColin and Vermote, 2001). Figure 1a shows an RGB image of a test scene acquired over Brazil not corrected for aerosol; Figure 1b shows the surface reflectance product for that same scene.

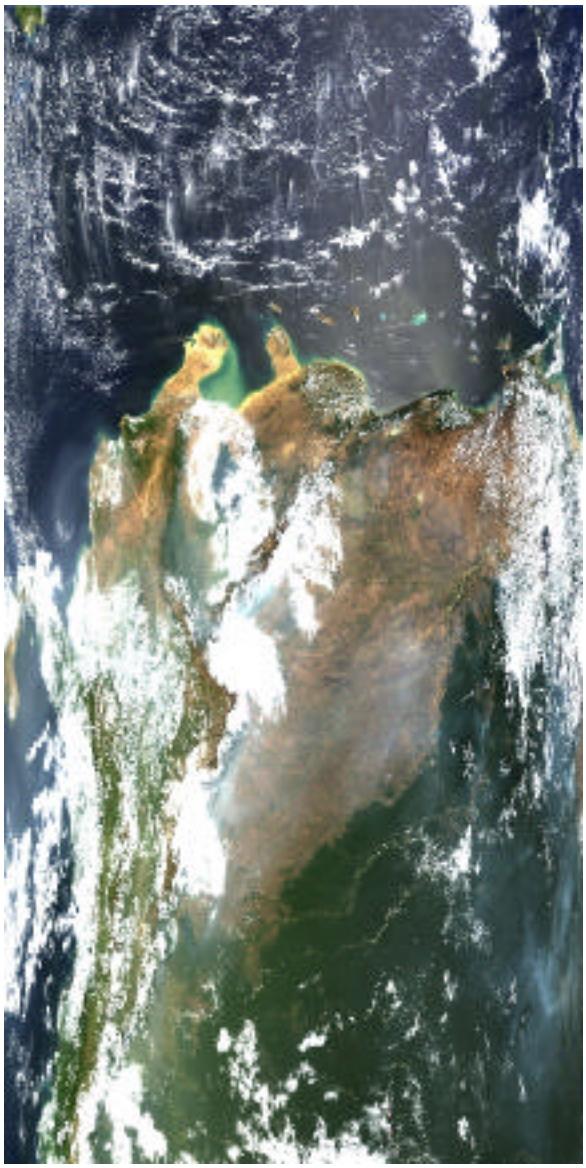

Figure 1a: RGB images of MODIS acquired over South America (Brazil and Bolivia) on March 12, 2001

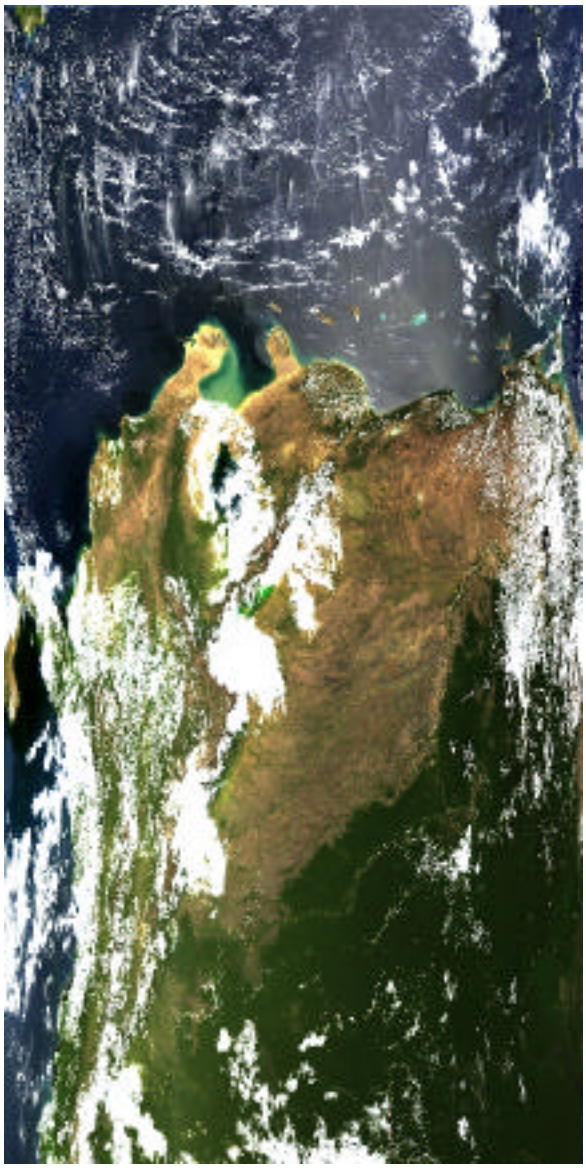

Figure 1b: RGB composite of the surface corresponding to Figure 1a.

On this day, the aerosol contamination was high, as illustrated by the visual differences between figure 1a and 1b. Large smoke plumes of optical thickness up and above 2.0 at 0.5mic were present on the scene.

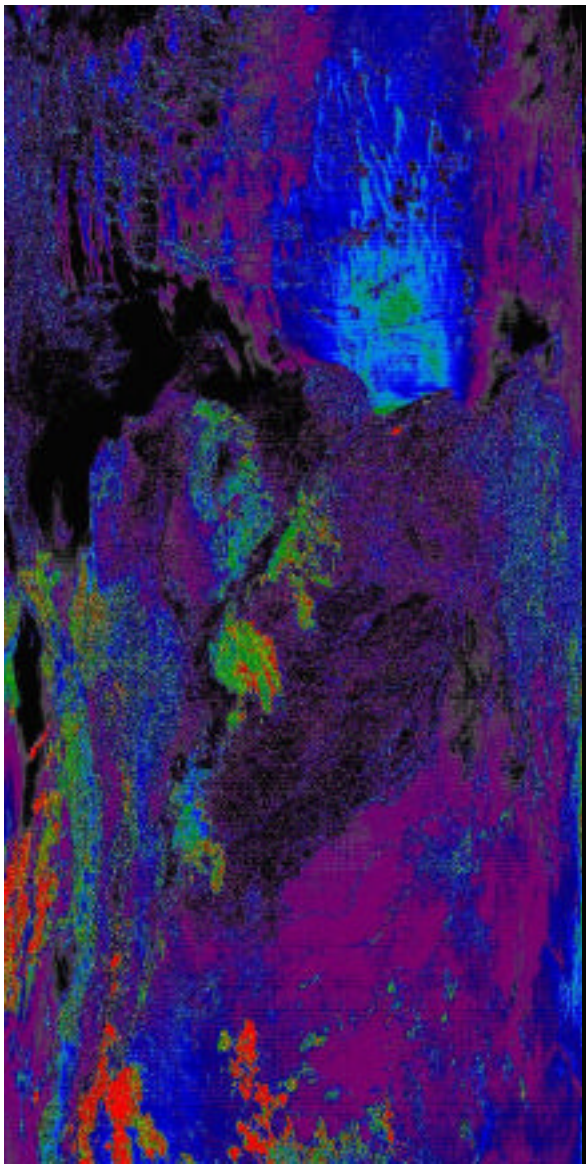

Figure 2a: Color image of MIRA scaled between **0**.03 (black) and 0.15 (red) reflectance unit

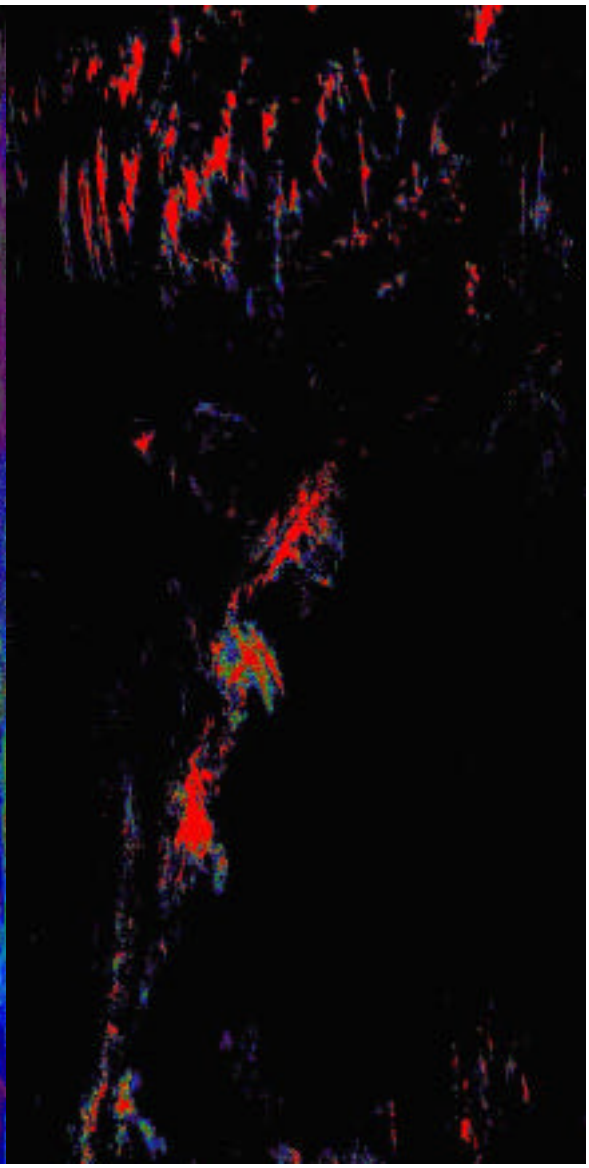

Figure 2b: Color image of band 26 (1.38mic) scaled between 0.015 (black) and 0.03 (red)

.

Figure 2a shows a false color image of the Middle Infrared reflectance anomaly in reflectance unit, with the scaling done between 0.03 (black) and 0.15 (red). When comparing to Figure 1a and 1b, one can see the higher values of MIRA (light blue to red) are obtained over clouds and sunglint, smoke, bright land surface or clear ocean, which does not produce any substantial middle infrared anomaly. Figure 2b shows the second quantity used to detect cloud in the internal cloud mask: the reflectance at 1.38mic (band 26). The reflectance is scaled between 0.015 and 0.03. One can see that MIRA and the 1.38mic reflectance are very complementary for detecting clouds. MIRA is very efficient in detecting low or high reflective cloud; 1.38mic is less efficient is detecting low cloud but very effective in detecting high cloud even if they are not very reflective. To improve the robustness, those reflective tests are coupled with a temperature test, where apparent surface temperature is computed using the Ocean split window technique and compared to the temperature of the air at 2m computed by the NCEP model every 6 hours (a simple temporal interpolation is done to NCEP data to bring them to the time of MODIS observation). The temperature derived from MODIS is presented on Figure 3a, and we can notice the lower temperature observed over some clouds. On the NCEP data the lowest temperature observed corresponds to higher elevation. Figure 3c presents the quantities used to confirm the cloud presence that is the difference between the surface temperature and the air temperature. With the difference scaled between –10K and 0K, one can see how nicely the simple difference captured the clouds present in that scene. Finally, figure 4b shows the final cloud analysis after the aerosol correction, and all tests are completed by an analysis of the residual anomaly in the visible (Blue –Red/2) conducted using the 500m bands after the aerosol correction. This test enables us to eliminate very small cloud or pixels not identified, but rejected in the aerosol inversion for other reasons (e.g. brighter surfaces).

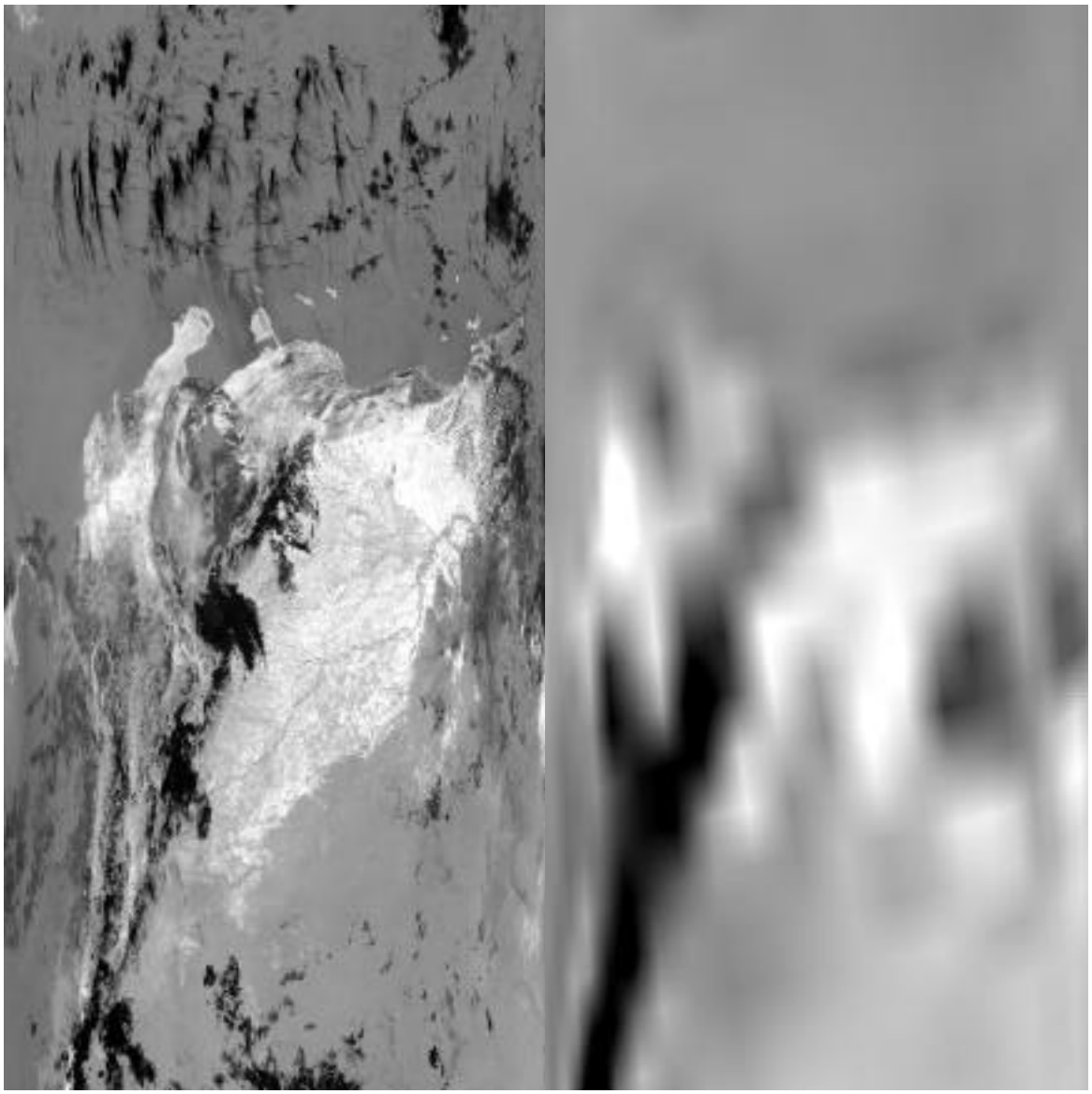

Figure 3a: Surface temperature derived from MODIS Scaled between 275K (black) and 323K (white)

Figure 3b: Air temperature from NCEP same scaling as Figure 3a.

Figure 4a: Surface temperature – air temperature Scaled between –10K (black) and 0K (white)

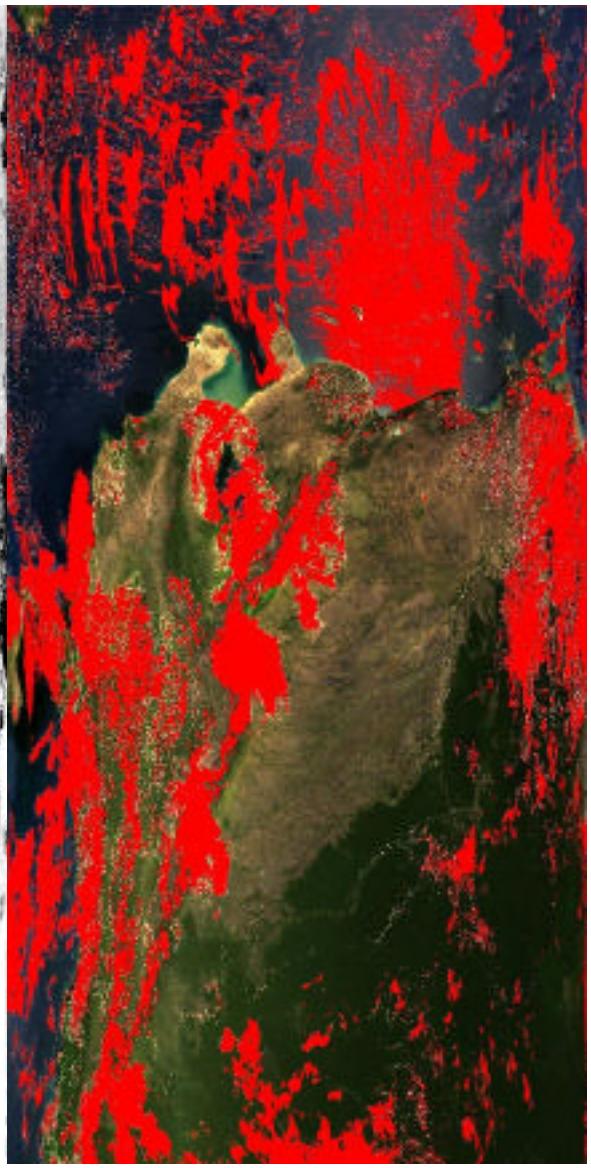

Figure 4b:Final cloud mask obtained after the aerosol correction.

Roger J.C and **Vermote E. F.,** 1998, A method to Retrieve the Reflectivity Signature at 3.75µm from AVHRR data, *Remote Sensing of the Environment*, 64:103-114.

PetitColin F. and Vermote E. F. 2001, Land surface reflectance, emissivity and temperature from MODIS middle and thermal infrared data, submitted to R.S.E.

1.2 Internal fire mask

An internal fire mask has also been implemented in the surface reflectance algorithm, basically based on one of the direct application of the surface reflectance in the middle-infrared. The fire mask has its own use for aerosol, and big fires can pertubate the signal at 2.13mic, which is used to estimate the reflectance in the visible (see previous report). It is therefore cautious to reject pixels that may be affected from fire from the aerosol inversion process. Figure 5 gives for the same scene again an illustration of the mechanism used to detect fire in the middle infrared. Figure 5 is an RGB image of the details of the previous scene; reflectance at 4.0mic (band 20 or 21) is in the red channel, 2.1mic in the blue channel, and 1.6mic in the green. Clouds detected previously are the blue features. Fires appear as red spots because the thermal anomaly produced by fires raised significantly the reflectance in the middle infrared (4.0mic) before it affects the shorter wavelengths (2.1mic and 1.6mic). For the filtering technique, we used the MIRA index once again, and we classified as fires the pixels where MIRA is greater than 0.1, which were not detected as clouds and those temperatures are greater than the air temperature. The difference between surface temperature and air temperature for fire detection is dependent on the geometry because specular reflectance can also cause elevated values of MIRA. The threshold in temperature difference is therefore dependent on the actual reflectance of the sunglint computed using geometry and NCEP surface winds. In the area where the sun-glint is significant (reflectance of glint > 0.05 at 2.1mic), fires are required to be at least 7.5K warmer than the air temperature, in other areas only a –5K difference is required.

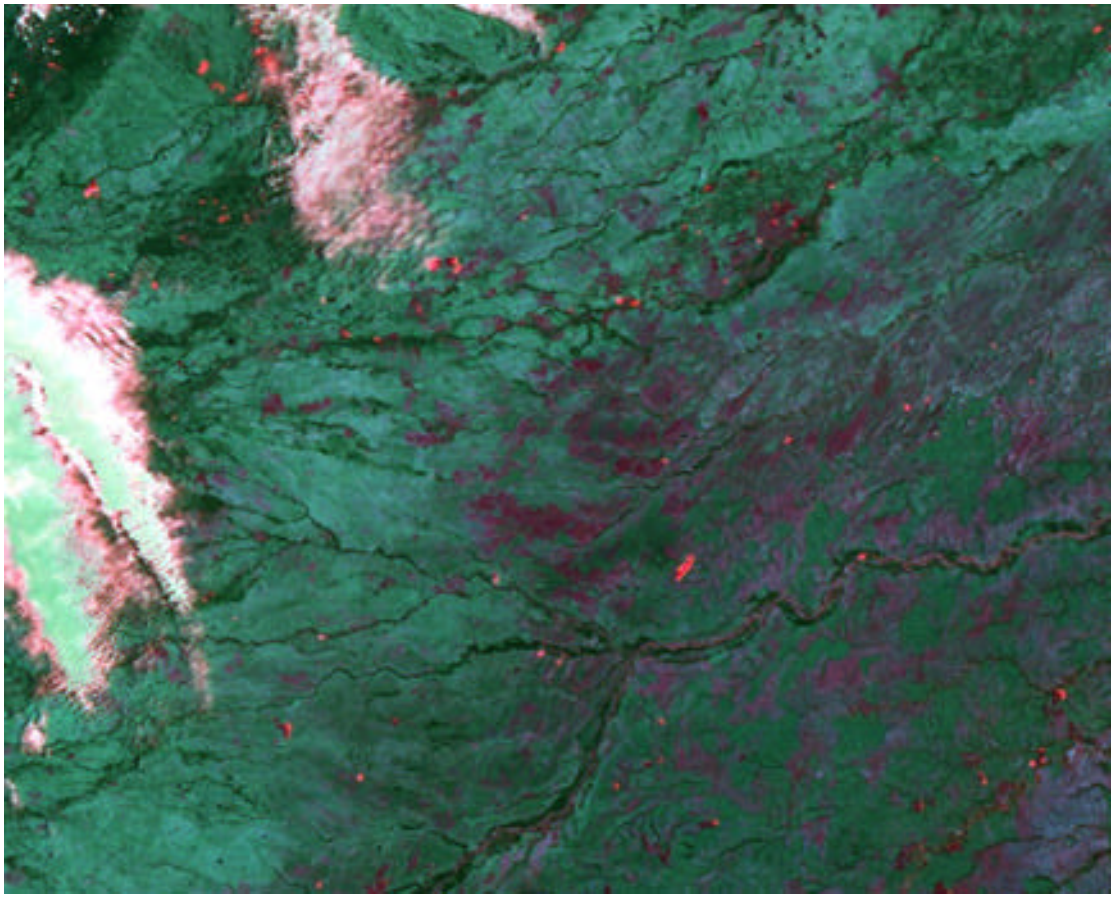

Figure 5a: Middle infrared RGB composite showing the reflectance observed at 4.0mic (Red), 1.6mic (Green) and 2.1mic (Blue) of details of the South America scene. Fires appear as small red clusters.

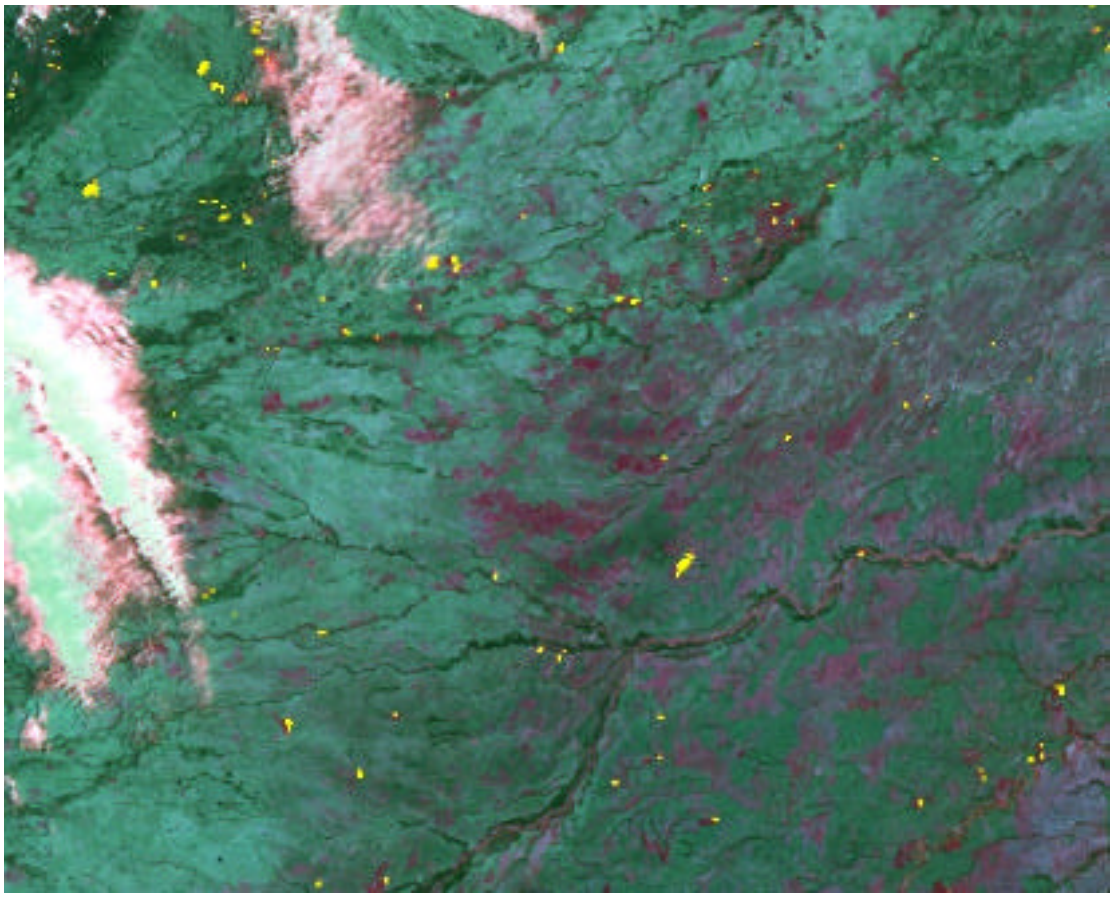

Figure 5b: Same as figure 5a, with the pixels detected by the internal fire mask are in yellow.

1.3 Internal sun-glint mask

Sun-glint is also detected, which is especially important over land where small bodies of water or water not in the land/water mask can be misinterpreted in fires, clouds or clear land pixels categories. The sunglint reflectance is computed dynamically over all surfaces (land and ocean). Over land when the reflectance of sun-glint is over 0.05, the pixels appear contaminated by sun-glint, showing a MIRA value above 1000 but not cold enough to be cloud and not hot enough to be fire and are flagged accordingly. Figure 6a illustrates the effect of sun-glint in the middle infrared RGB

composite; figure 6b shows the masking of the sun-glint according to the criteria described above.

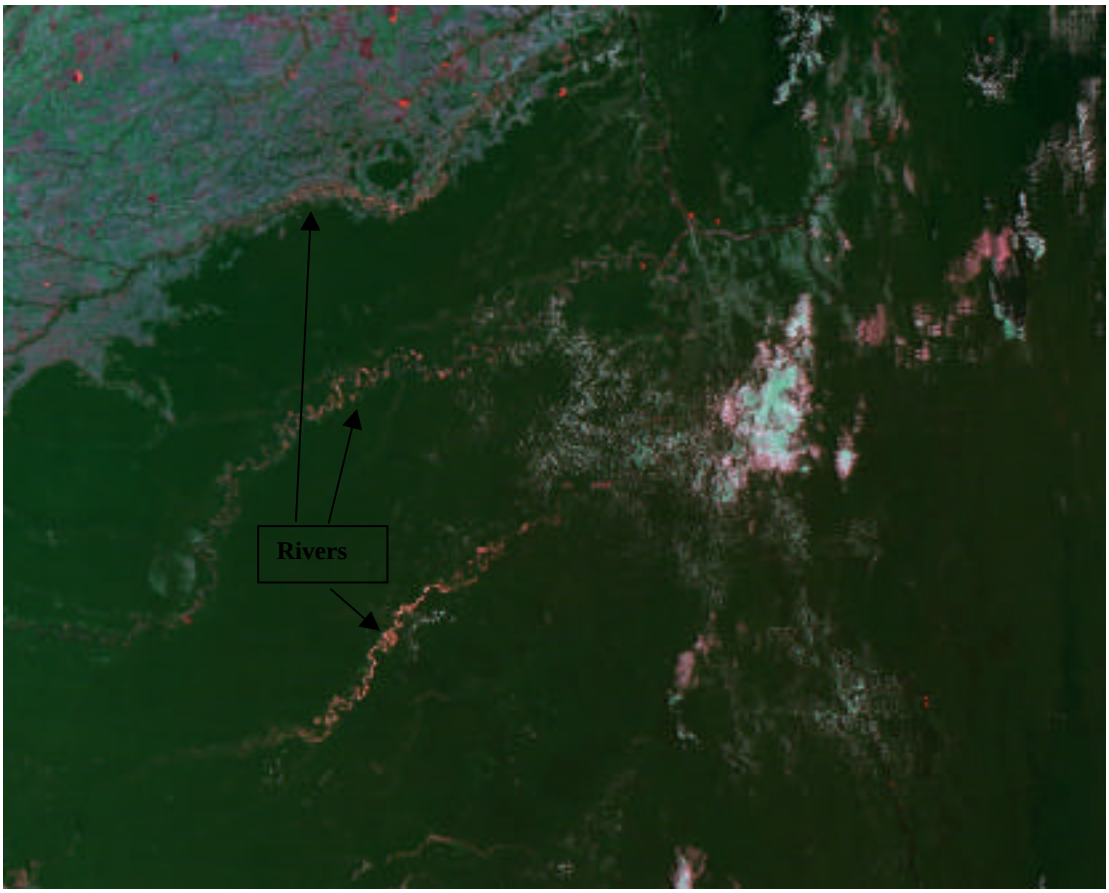

Figure 6a: Details of the South America scene presented in the middle infrared RGB, the river appear reddish because they are affected by sun-glint.

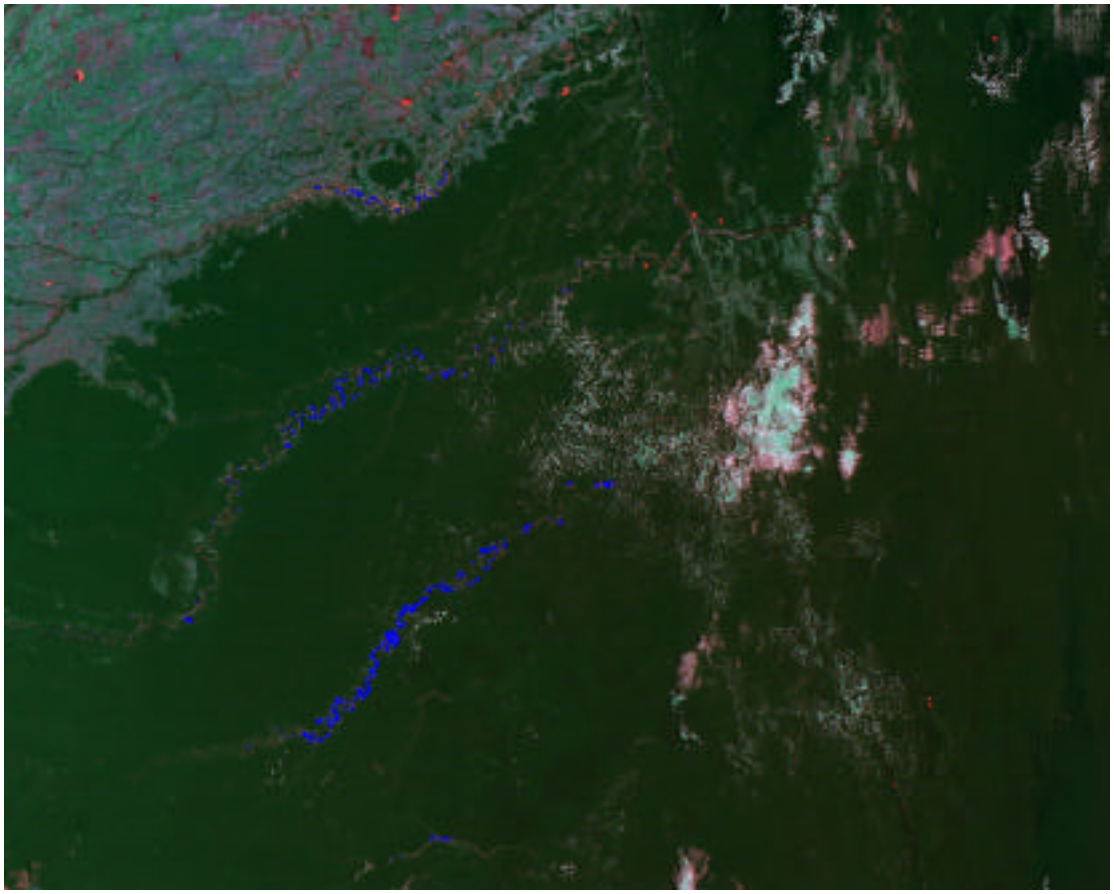

Figure 6b: Same as figure 6a, but the sun-glint mask has been applied in blue.

1.4 Internal snow mask

The snow detection is important because snow can easily be confused with a “dark target” in the shortwave infrared. In the previous report, we have indicated these problems and set up some filtering criteria for snow. We are continuing to apply those criteria in an effort to discriminate between snow and cloud. When snow is detected, the aerosol algorithm performs an aggressive filtering of the optical thickness values (based on spectral dependence) around the snow-covered area to eliminate contamination by sub-pixel snow as much as possible. It is therefore important to limit that process as much as possible to optimize processing time and reduce “false” rejection. The internal cloud mask described previously should not misclassify snow as cloud because it uses quantities that are not sensitive to snow (MIRA and band 26) in most conditions (i.e.

band 26 may show a response to snow at higher altitude but this problem is being addressed by increasing the threshold on band 26 as a function of altitude). Therefore, for pixels which have not been classified as cloud, fire or sunglint, but still have a high visible reflectance anomaly (blue-red/2) the test using the ratio between band 5 (1.24mic) and 2 (0.87mic) is used classify the pixels as snow or not, and in addition a condition on the surface temperature (Ts should be <280K) is also required.

Figure 7a shows a true RGB of the scene of interest to demonstrate our snow filtering. The scene is partially covered by snow and cloud; in the visible it is difficult to clearly discriminate between the two in most cases. Figure 7b, shows a false RGB that makes discrimination easier; in this RGB the snow appears now as very dark blue, since the reflectance of snow is small at 1.6mic and 4.0mic (or even 2.13mic) but very high in the visible (0.47mic). The low altitude cloud of water droplets are more or less white or sometimes the higher altitude clouds that contain ice particles are blue but of lighter tint than snow. Qualitatively this composite gives us a good indication of where snow is and where clouds may contaminate the scene. Figure 7c, shows the internal snow mask, and it appears to correctly detect most of the snow without problems, but there are a few cases where the cirrus band causes snow to be classified as cloud (on mountains tops), but is seems very limited. For the intended purposes, the internal snow mask is very satisfactory.

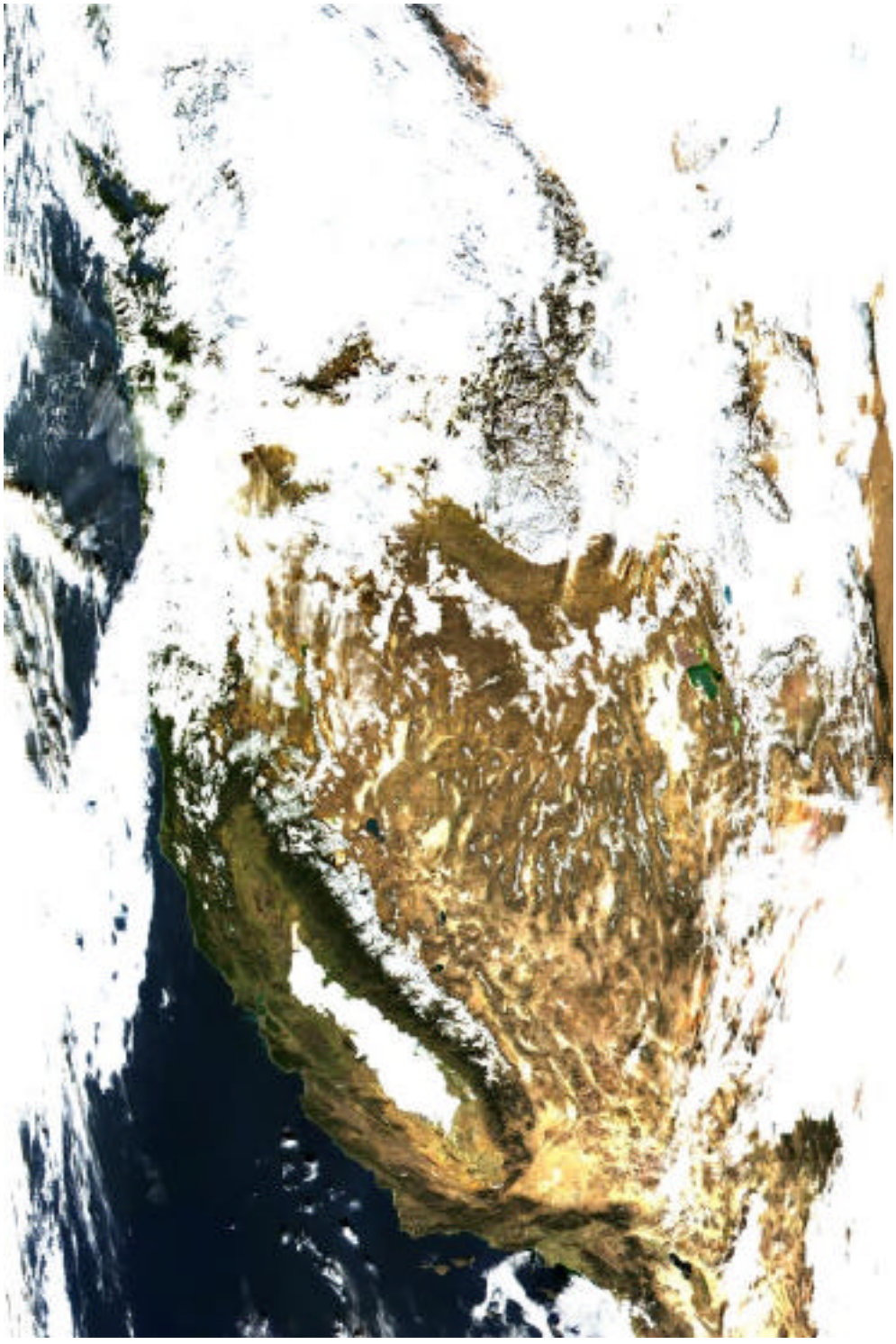

Figure 7a: True RGB image of a MOD09 granule over the US west coast on day 337 (2000).

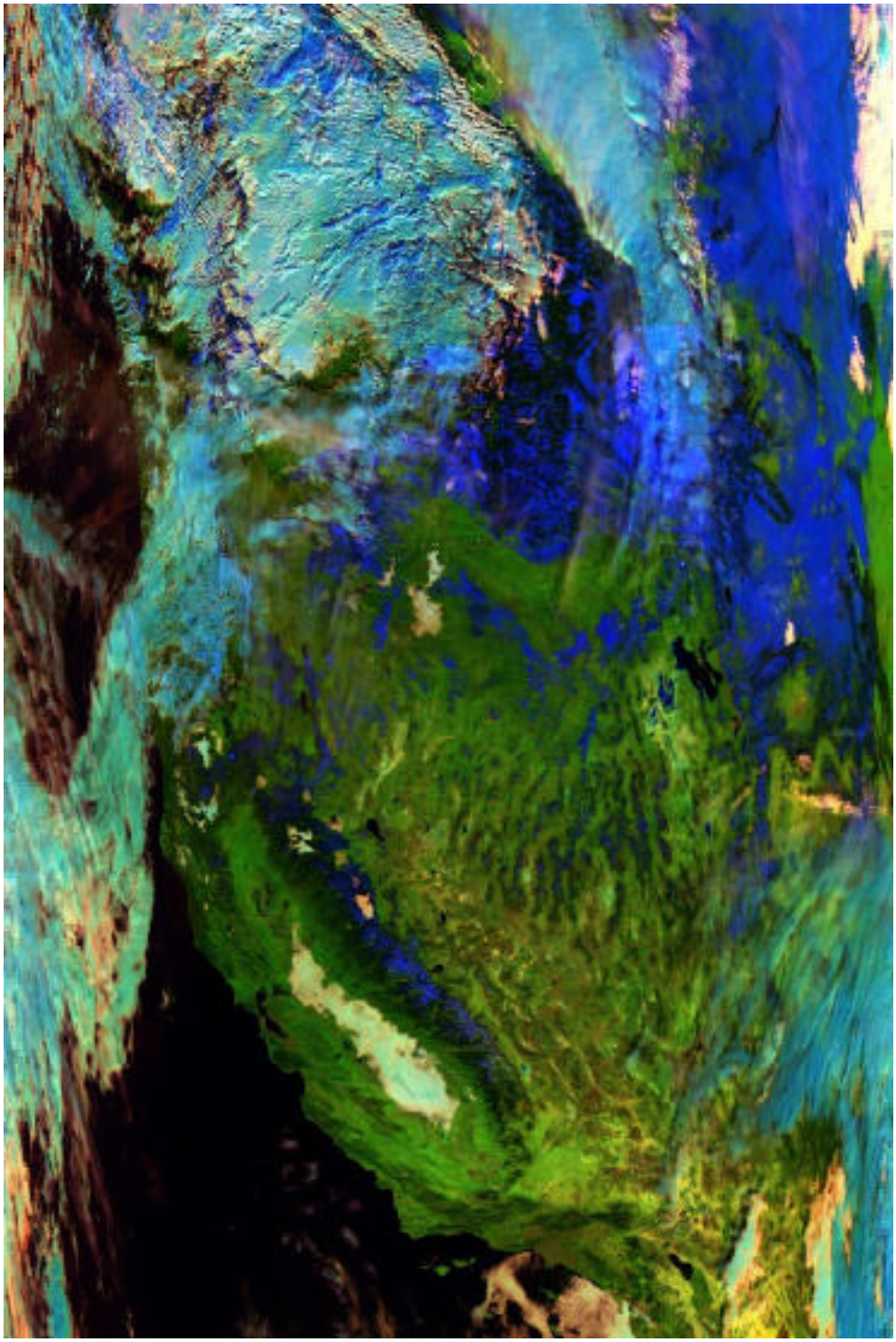

Figure 7b: False RGB (Red=4.0mic,Green=1.6mic,Blue=0.47mic) corresponding to figure 7a.

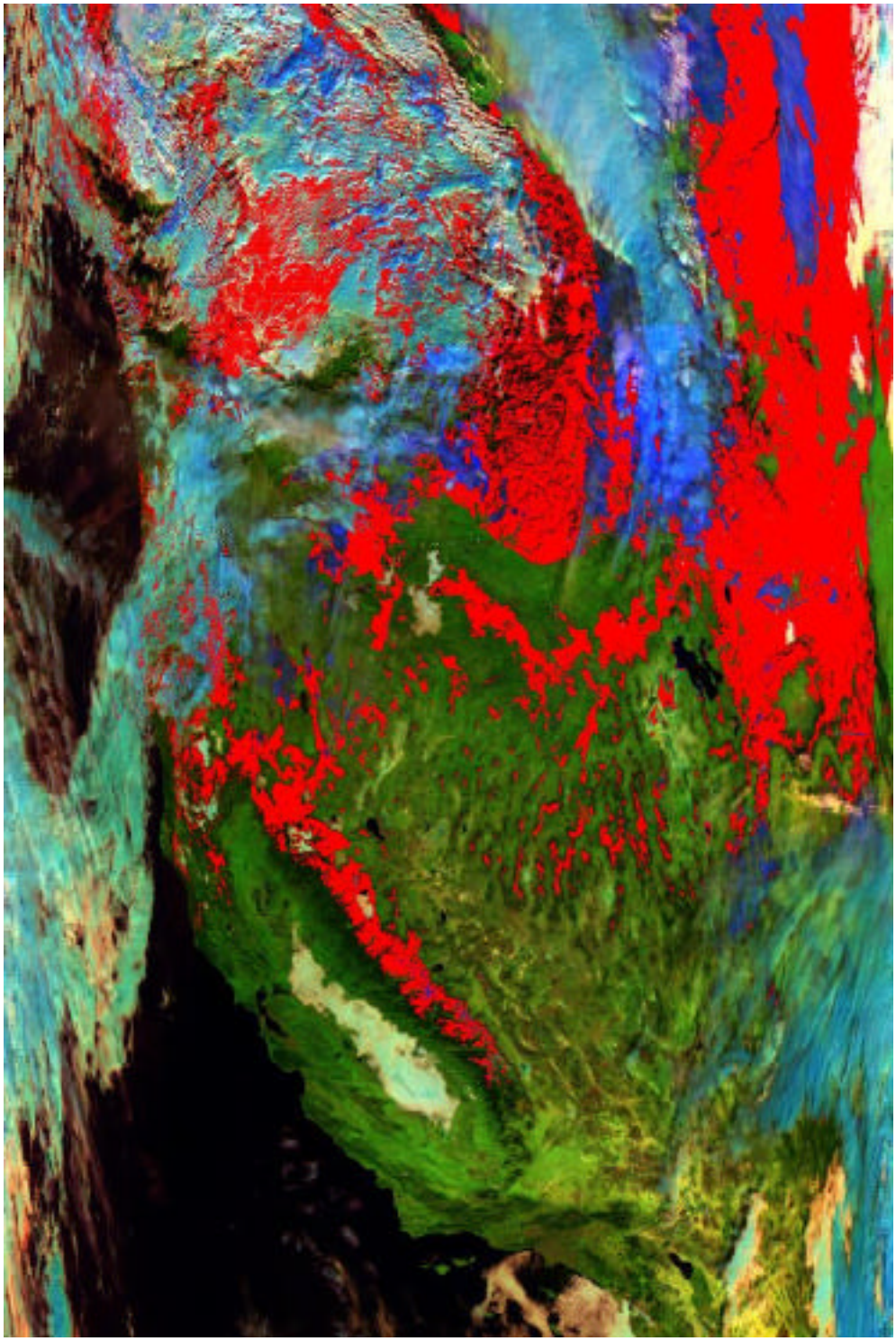

Figure 7c: Results of the internal snow mask (snow is in red), corresponding to figure 7a and figure 7b.

3. Middle infrared surface reflectance

Our goal is the retrieval of the land surface reflectance in the middle infrared (3.5-4.2μm – MODIS band 20 to 23). During the first semester of year 2001, the processing tools for the retrieval of the middle infrared surface reflectance have been improved thru an analysis of the results. A database of middle infrared surface reflectance is being built. Two applications, where the middle infrared surface reflectance brings a new perspective, were investigated. They are the retrieval of emissivity in middle and thermal infrared and the fire detection.

3.1 Analysis of middle infrared surface reflectance

Figure 8 shows surface reflectances in MODIS band 20 over Southern Africa for granule 2000-238-0855. Middle infrared surface reflectances present high values over bare soils and decrease as the density of the vegetation cover increases. Surface reflectances over water are very low. Analysis of the middle infrared surface reflectance derived over southern Africa during the period of time starting August 20th, 2000 and ending September 4th, 2000 shows that the accuracy is sufficient to capture angular variations of the reflectance as illustrated in Figure 8. The Bidirectional Reflectance Distribution Function (BRDF) model developed for the MODIS BRDF product has been applied to fit the surface reflectances. Very high middle infrared surface reflectances occur sporadically. Further analysis indicates that such high reflectances are due to the presence of fire within the pixel.

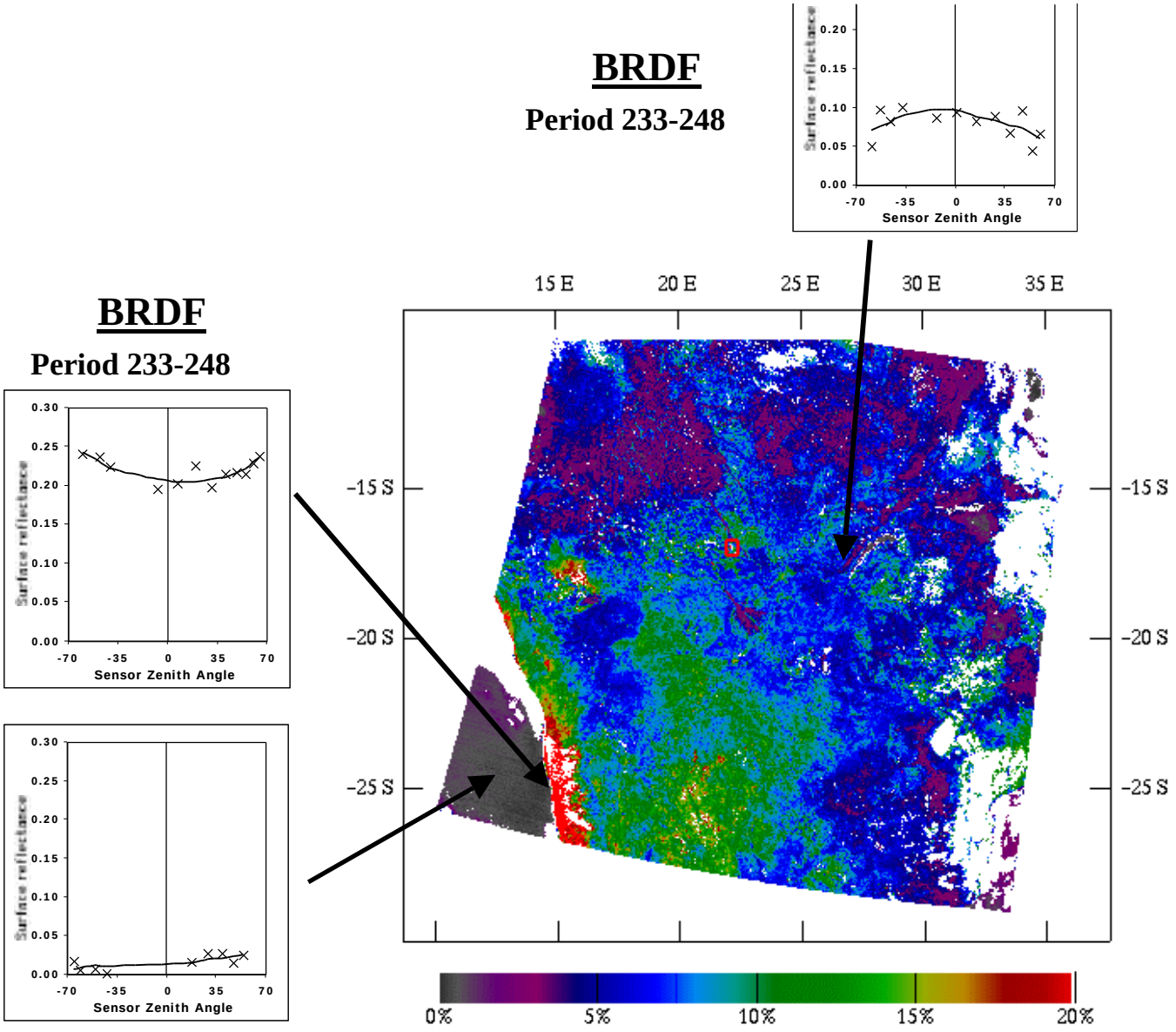

Figure 8: Surface Reflectance in MODIS band 20 for one granule (2000-238-08:55) and angular variations recorded during the time period 2000-233 to 248 with associated BRDF model results.

3.2 Improvements of the processing tools for the middle infrared surface reflectance retrieval

The selected method for middle infrared surface reflectance retrieval involves radiometric measurements in the middle infrared and in the thermal infrared (10 – 12μm – MODIS bands 31), as well as day-time and night-time observations. The development of a data processing prototype, in order to demonstrate the feasibility of the separation between thermal emission and solar reflection in the middle infrared spectrum, has been engaged for several months (see previous reports). The prototype has been improved in two ways: a) temporal interpolation of the atmospheric profiles for better atmospheric corrections; and b) adaptive spatial sampling technique when nighttime and daytime data are compared.

To correct the brightness temperatures recorded by the MODIS sensor from the atmospheric perturbation, the MODTRAN radiative transfer code is fed by atmospheric data provided every six hours by the National Center for Environmental Prediction (NCEP). Originally, atmospheric corrections of a single MODIS granule were performed with the closest atmospheric data in time. In some cases, local atmospheric conditions changed rapidly and middle infrared surface reflectances with significant bias were revealed. In order to reduce such errors, the two atmospheric data sets that bracket the granule acquisition time are now considered and a new set of atmospheric profiles, corresponding to the actual data acquisition time, are generated by linear interpolation. Averaged Temperature Independent Spectral Indices of Emissivity (TISIE) are derived from time series of nighttime acquisitions and are introduced in the derivation of the

middle infrared surface reflectance from day-time data. Averaging 16 days of night-time TISIE and using the result with day-time data raise a projection issue as the exact location and size of the MODIS pixel over the same area vary from one acquisition to another. The adaptive spatial sampling approach adopted is illustrated in Figure 9 and is based on the sampling technique currently applied in the MODIS production system. A geographical map with a spatial sampling of 0.01 degree in latitude and longitude has been adopted as a reference map. Once central geolocation and size of the MODIS pixel are computed, all cells in the reference map, covered entirely or partially by the MODIS pixel, are updated with regard to the TISIE, with a specific weight w_t . This weight takes into account the fraction of the cell covered by the MODIS pixel and the fraction of the MODIS pixel that is common with the cell.

3.3 A database of middle infrared surface reflectance

As the stability of the middle infrared surface reflectance retrieval improved, intensive data analysis started. The need of a database of middle infrared surface reflectance, or a database including any data needed to produce such reflectance, for validation, BRDF or time-series analysis was visible. In the early phase, the database was limited to Southern Africa (south of 10 degree South), starting August 20th, 2000. In a second phase, with MODIS data acquired after November 12th, 2000, the database was extended to the whole African continent, Europe and the Middle East. A few weeks later, data over the Australian continent were added to the database.

The database includes NCEP ancillary data, geolocation product (MOD03) and measured radiances in MODIS bands 20-23, 29, 31 and 32 extracted from the MOD021KM product. Such data were downloaded from the MODAPS system, as they were available. The database includes also atmospheric parameters files, maps of TISIE and maps of BRDF model parameters. Granules of middle infrared surface reflectance are not stored in the database as they are easy to produce from level 1B data, atmospheric parameter files and corresponding maps of TISIE. Data processing and archiving are performed at the MODIS surface reflectance Science Computing Facility (SCF).

3.4 Applications of the middle infrared surface reflectance

Among many applications, the middle infrared surface reflectance offers new perspectives for land emissivity retrieval and fire detection and characterization. Applying the Kirchhoff's law, derivation of directional emissivity from BRDF in the middle infrared is straightforward. Then, using emissivity ratios, directional emissivity in other MODIS land thermal bands (29, 31 and 32) is computed. Results over Southern Africa for the 16-day time period starting August 20th, 2000 are presented in Figure 10. In order to check the consistency of spectral emissivities, land surface temperatures retrieved at different wavelength were compared. Two types of comparisons were performed: one regional with surface temperatures from an area of a single granule (September 1st, 2000) with large surface temperature range, and one temporal with time series of night-time and day-time surface temperatures over three locations in Southern Africa during two months. Results of the comparisons are summarized in Table 1. All standard deviations between surface temperatures retrieved at different wavelength are less than 1.5 degree Kelvin. Such good results show a good consistency

with regard to the surface temperatures and, indirectly, a good consistency of the emissivities.

BAND (μm)	20 (3.79)	22 (3.97)	23 (4.02)	29 (8.53)	31 (11.02)	32 (12.03)	
20		0.45	0.51	0.53	0.40	0.49	
22	0.59		0.54	0.56	0.47	0.55	Regional Analysis
23	0.81	0.60		0.44	0.52	0.62	
29	0.85	1.19	1.12		0.36	0.44	
31	0.46	0.77	0.85	1.29		0.20	
32	0.61	0.89	0.96	1.46	0.59		
	Temporal Analysis						

Table 1: Standard deviation between land surface temperatures computed in MODIS bands 20, 22, 23, 29, 31 and 32 for the regional and temporal analysis.

Regarding fire detection, a simple detection algorithm was established by comparing surface reflectances in MODIS band 20 and 7 (2.1mm). Such a technique is simple and keeps the radiometric information related to fires available for further study such as the retrieval of fire size and temperature. Comparisons with ASTER data have been engaged in this way.

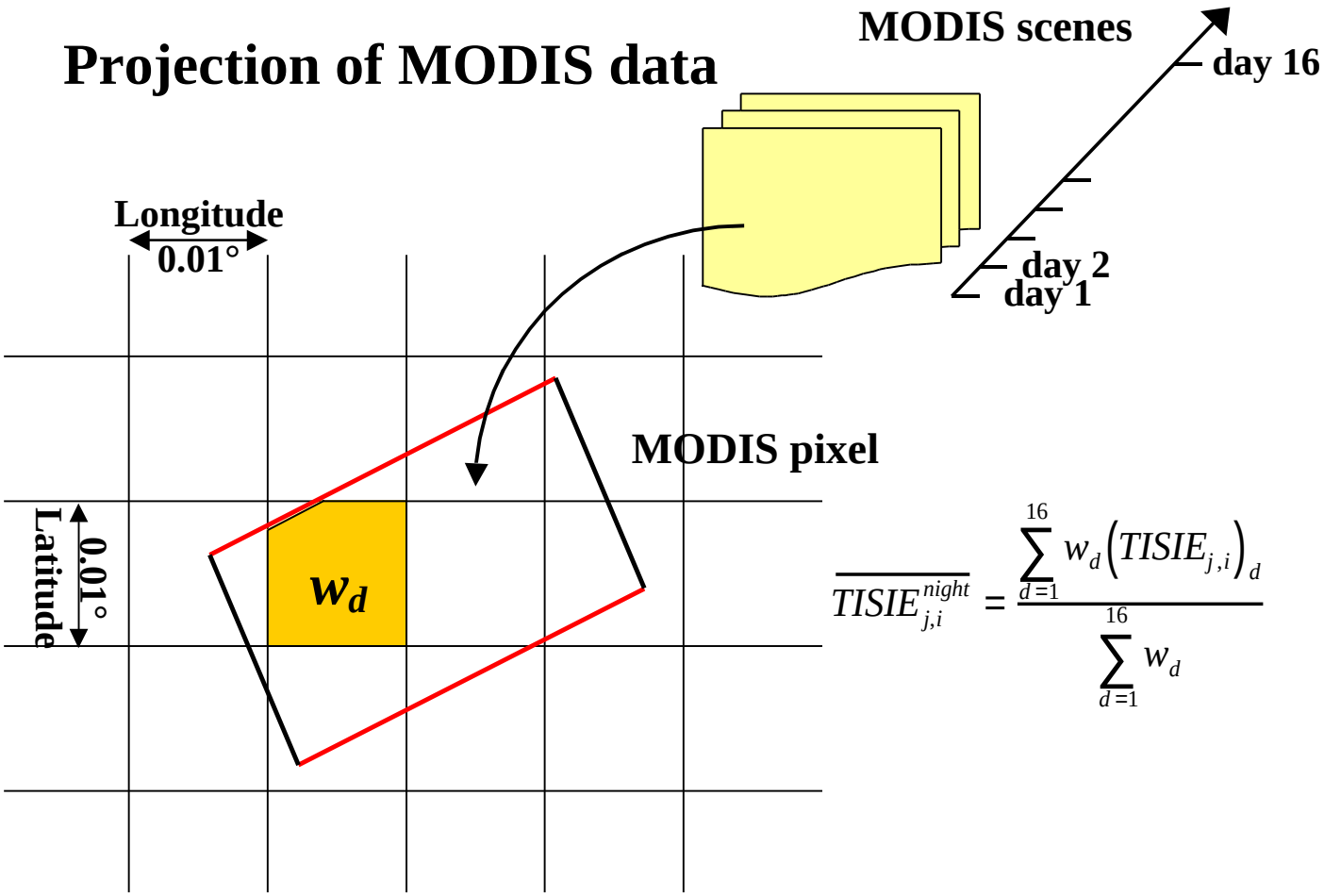

.

Figure 9: TISIE averaging with adaptive spatial sampling technique.

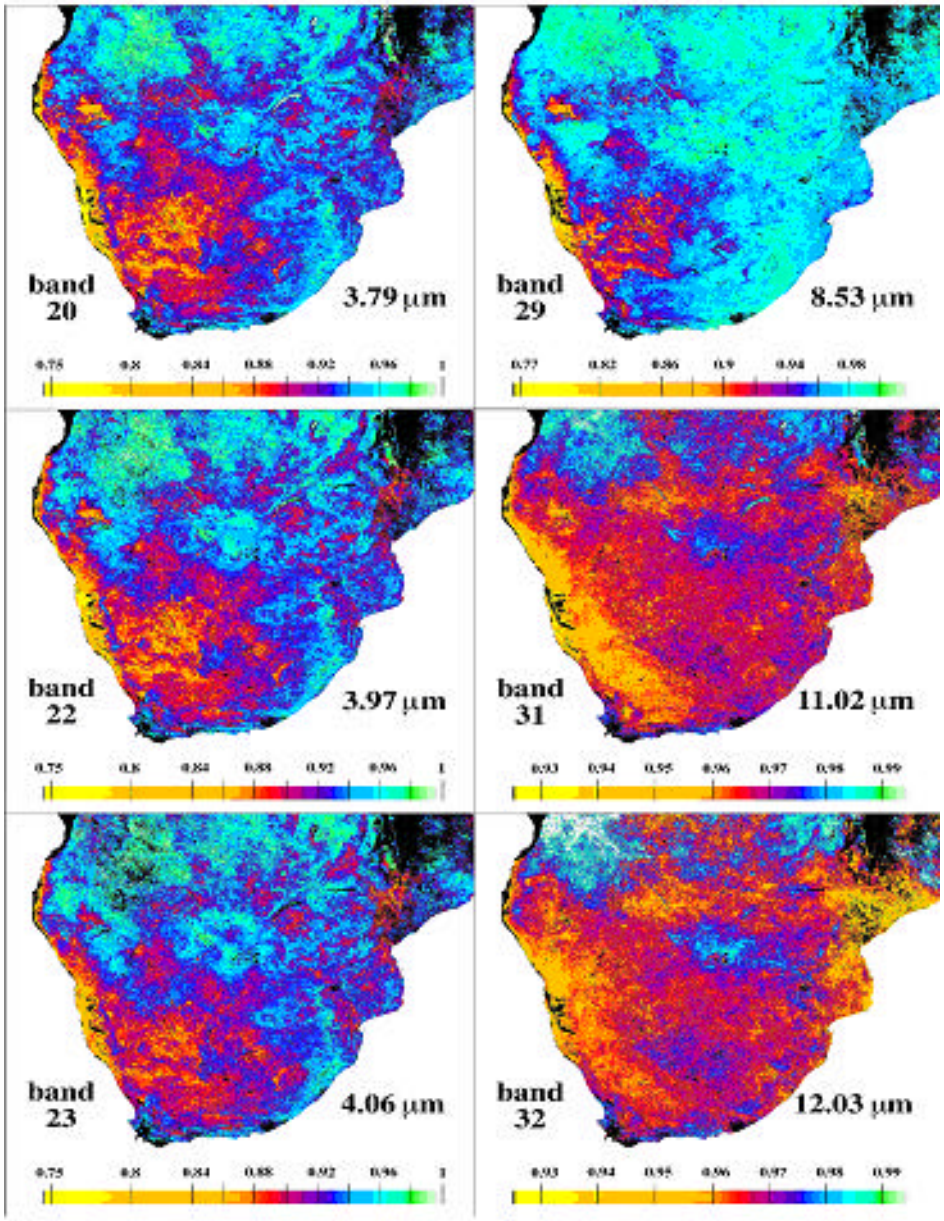

Figure 10: Maps of nadir emissivity over Southern Africa for the 16 days time period starting August 20th 2000 for MODIS middle and thermal infrared land bands

4.0 MODIS Adaptive Processing System (MODAPS) / PI Processing /250m system

The Land surface reflectance SCF remains actively involved in the PI-led processing activity ranging from making sure that PIs' needs are accurately perceived by the MODAPS development team and by management, as well as participating in the development of the processing system and various phases of testing.

The SCF participated in the weekly PI-Processing meetings where Eric Vermote represented the land group.

The SCF also participated in all of the weekly MODAPS meetings/telecons, where problems were discussed to identify solutions and where progress in the new development was tracked.

Following the SWAMP recommendation to ensure the production of global MODIS data, our SCF participated in the discussions to identify alternatives to the 0.5X MODAPS original production plan. The solution that was adopted was to take the production of the 250m out of MODAPS. A completely independent system generates 10% of the 250m land surface reflectance and VI's so as to provide some data for the PI's to evaluate (see http://modis-250m.nascom.nasa.gov/). Our SCF played an important role in the shaping of this proposal and in building the prototype production system.

B. **MEETINGS ATTENDED**

- MODIS Science Team Meeting (Jan, 01) Columbia.
- Weekly PI Processing Status Meetings, NASA/GSFC.
- Weekly Technical Team Meetings, NASA/GSFC.
- Weekly SDDT (Science Data Discipline Team) Meetings.
- Weekly MsWG (MCST Science Working Group) Meeting